

# Regulation of reconstituted high density lipoprotein structure and remodeling by apolipoprotein E

Kerry-Anne Rye,<sup>1,\*,\dagger,\S</sup> Richard Bright,<sup>\*</sup> Maria Psaltis,<sup>\*</sup> and Philip J. Barter,<sup>\*,\dagger</sup>

Lipid Research Group,<sup>\*</sup> The Heart Research Institute, Camperdown, Sydney, New South Wales, Australia 2050; Department of Medicine,<sup>\dagger</sup> University of Sydney, New South Wales, Australia 2006; Department of Medicine,<sup>\S</sup> University of Melbourne, Victoria, Australia 3010

**Abstract** Apolipoprotein E (apoE) enters the plasma as a component of discoidal HDL and is subsequently incorporated into spherical HDL, most of which contain apoE as the sole apolipoprotein. This study investigates the regulation, origins, and structure of spherical, apoE-containing HDLs and their remodeling by cholesteryl ester transfer protein (CETP). When the ability of discoidal reconstituted high density lipoprotein (rHDL) containing apoE2 [(E2)rHDL], apoE3 [(E3)rHDL], or apoE4 [(E4)rHDL] as the sole apolipoprotein to act as substrates for LCAT were compared with that of discoidal rHDL containing apoA-I [(A-I)rHDL], the rate of cholesterol esterification was (A-I)rHDL >> (E2)rHDL ~ (E3)rHDL > (E4)rHDL. LCAT also had a higher affinity for discoidal (A-I)rHDL than for the apoE-containing rHDL. When the discoidal rHDLs were incubated with LCAT and LDL, the resulting spherical (E2)rHDL, (E3)rHDL, and (E4)rHDL were larger than, and structurally distinct from, spherical (A-I)rHDL. Incubation of the apoE-containing spherical rHDL with CETP and Intralipid<sup>®</sup> generated large fusion products without the dissociation of apoE, whereas the spherical (A-I)rHDLs were remodeled into small particles with the formation of lipid-poor apoA-I. **In conclusion,** i) apoE activates LCAT less efficiently than apoA-I; ii) apoE-containing spherical rHDLs are structurally distinct from spherical (A-I)rHDL; and iii) the CETP-mediated remodeling of apoE-containing spherical rHDL differs from that of spherical (A-I)rHDL.—Rye, K.A., R. Bright, M. Psaltis, and P.J. Barter. **Regulation of reconstituted high density lipoprotein structure and remodeling by apolipoprotein E.** *J. Lipid Res.* 2006. 47: 1025–1036.

**Supplementary key words** cholesteryl ester transfer protein • apolipoprotein A-I • kinetics

The HDLs in human plasma have been classified on the basis of their two main apolipoproteins, apolipoprotein A-I (apoA-I) and apoA-II, into two major subpopulations of particles: those that contain apoA-I without apoA-II, and those that contain both apoA-I and apoA-II (1). These subpopulations have been the subject of intense investigation

for many years, and their structure, function, and metabolism are well understood. However, up to 10% of the HDLs in human plasma contain neither apoA-I nor apoA-II but have apoE as their main apolipoprotein constituent (2–4). Despite the fact that ~75% of the apoE in normal human plasma is associated with HDL (5) and that the antiatherogenic properties of this apolipoprotein are well documented, remarkably little is known about the structure, origins, or metabolism of apoE-containing HDLs. This paper addresses these issues.

ApoE is a 34.2 kDa, 299 residue protein that consists of a 22 kDa N-terminal receptor binding domain and a 10 kDa C-terminal lipid binding domain (6). Three apoE isoforms with cysteine/arginine interchanges at positions 112 and 158 have been identified in human plasma (7, 8). Whereas apoE2 and apoE4 have cysteine and arginine residues at both of these positions, apoE3 has a cysteine residue at position 112 and arginine at position 158.

ApoE is synthesized in the liver and enters the plasma predominantly as a component of discoidal HDL (9). Once in the plasma, apoE is rapidly incorporated into spherical HDL (diameter, 9.0–18.5 nm) (2). When HDLs from normolipidemic plasma are subjected to two-dimensional gel electrophoresis (agarose gel electrophoresis followed by nondenaturing polyacrylamide gradient gel electrophoresis), almost no apoA-I or apoA-II comigrates with apoE (2–4). This suggests that most apoE-containing HDLs do not contain either apoA-I or apoA-II. Other investigators have reached the same conclusion using techniques such as gel filtration chromatography and isotachopheresis (5, 10).

To investigate the structure, origins, and metabolism of apoE-containing spherical HDL, it is important to have

Abbreviations: apoE, apolipoprotein E; CE, cholesteryl ester; CETP, cholesteryl ester transfer protein; DPH, 1,6-diphenyl-1,3,5-hexatriene; Gdn-HCl, guanidine hydrochloride; PRODAN, 6-propionyl-2-(dimethylamino)-naphthalene; rHDL, reconstituted high density lipoprotein; Sulfo-EGS, sulfo-ethylene glycol bis[sulfosuccinimidylsuccinate]; TG, triglyceride; TMA-DPH, 1-(4-trimethylammoniumphenyl)-6-phenyl-1,3,5-hexatriene *p*-toluenesulfonate; UC, unesterified cholesterol.

<sup>1</sup>To whom correspondence should be addressed.

e-mail: ryek@hri.org.au

Manuscript received 1 December 2005 and in revised form 12 January 2006 and in re-revised form 1 February 2006.

Published, *JLR Papers in Press*, February 1, 2006.  
DOI 10.1194/jlr.M500525-JLR200

Copyright © 2006 by the American Society for Biochemistry and Molecular Biology, Inc.

This article is available online at <http://www.jlr.org>

access to substantial amounts of discoidal and spherical particles that are uniform in size and composition and contain apoE as the sole apolipoprotein. As it is not possible to isolate sufficient amounts of these HDLs from plasma, well-characterized preparations of discoidal and spherical reconstituted high density lipoprotein (rHDL) containing recombinant apoE2 [(E2)rHDL], apoE3 [(E3)rHDL], or apoE4 [(E4)rHDL] as the sole apolipoprotein were used for the current project.

The results show that LCAT converts discoidal (E2)rHDL, (E3)rHDL, and (E4)rHDL into spherical particles that are structurally distinct from each other, as well as from spherical rHDL containing apoA-I [(A-I)rHDL]. They also establish that cholesteryl ester transfer protein (CETP) remodels apoE-containing spherical rHDL into large fusion products without the dissociation of apoE. This is in direct contrast with the CETP-mediated remodeling of spherical (A-I)rHDL, in which small particles are generated in a process that is accompanied by the dissociation of lipid-free or lipid-poor apoA-I.

## EXPERIMENTAL PROCEDURES

### Isolation of apoA-I, LCAT, and CETP

ApoA-I, LCAT, and CETP were isolated from pooled samples of expired, autologously donated human plasma (Gribbles Pathology, Adelaide, Australia) as described (11). The apoA-I was judged to be >95% pure when subjected to SDS-PAGE (Phast-Gel; Amersham Pharmacia Biotech) and staining with Coomassie Blue R-350.

LCAT activity was assessed using discoidal rHDL containing POPC (Sigma), unesterified cholesterol (UC) (Sigma), a tracer amount of [ $1\alpha,2\alpha$ - $^3\text{H}$ ]cholesterol ([ $^3\text{H}$ ]UC) (Amersham Pharmacia Biotech), and apoA-I as the substrate (12). The assay was linear as long as <30% of the [ $^3\text{H}$ ]UC was esterified. The LCAT used in this study generated 2,144 nmol of cholesteryl ester (CE)/ml LCAT/h.

CETP activity was assessed as the transfer of [ $^3\text{H}$ ]CE from [ $^3\text{H}$ ]CE-labeled HDL<sub>3</sub> to ultracentrifugally isolated LDL (13, 14). The assay was linear as long as <30% of the [ $^3\text{H}$ ]CE transferred from the HDL<sub>3</sub> to LDL. The activities of the CETP preparations used in this study ranged from 48 to 59 U/ml, where 1 unit is the transfer activity of 1 ml of a preparation of pooled, human lipoprotein-deficient plasma.

### Expression and purification of apoE2, apoE3, and apoE4

Vectors containing human apoE2, apoE3, and apoE4 cDNA were kindly provided by Dr. Karl Weisgraber (Gladstone Institute of Cardiovascular Disease, University of California, San Francisco, CA). ApoE2, apoE3, and apoE4 were expressed from *Escherichia coli* strain BL21-CodonPlus<sup>®</sup> (Stratagene, La Jolla, CA) as described (15, 16). The expressed proteins were chromatographed on Sephacryl S-300 (Amersham Pharmacia Biotech) and appeared as single bands when subjected to SDS-PAGE and silver staining.

### Preparation of discoidal and spherical (E2)rHDL, (E3)rHDL, (E4)rHDL, and (A-I)rHDL

Discoidal rHDLs containing POPC, UC, and apoE2, apoE3, apoE4, or apoA-I were prepared by the cholate dialysis method and converted into spherical rHDLs by incubation with LDL and LCAT (16, 17). Under these conditions, <10% of the LDL

phospholipids transferred to the rHDL (18). The spherical rHDLs were isolated by ultracentrifugation in the  $1.07 < d < 1.21$  g/ml density range. Unless stated otherwise, the discoidal and spherical rHDLs were dialyzed against  $3 \times 1$  liter of 0.01 M TBS (pH 7.4) containing 0.15 M NaCl, 0.005% (w/v) EDTA-Na<sub>2</sub>, and 0.006% (w/v) NaN<sub>3</sub> before use.

### Size-exclusion chromatography

Discoidal (E2)rHDL, (E3)rHDL, (E4)rHDL, and (A-I)rHDL (200  $\mu\text{g}$  of apolipoprotein in 200  $\mu\text{l}$  of TBS) were loaded individually onto a Superose 6 column (Amersham Pharmacia Biotech) and eluted with TBS at a flow rate of 0.5 ml/min. The absorbance of the eluate was monitored continuously at 280 nm. Protein standards of known diameter were also applied to the column and eluted under conditions identical to those used for the discoidal rHDL.

### Kinetic studies

Varying concentrations of [ $^3\text{H}$ ]UC-labeled discoidal rHDLs were mixed with BSA and  $\beta$ -mercaptoethanol, then incubated with a constant amount of LCAT (see figure legends for details). When the incubations were complete, the tubes were placed immediately on ice. UC was precipitated with digitonin (12), and the supernatants were counted in a Beckman LS 6000TA liquid scintillation counter (Beckman Instruments, Fullerton, CA). The kinetic parameters  $V_{max}$  and  $K_m$  (*app*) were determined by non-linear regression analysis (GraphPad Prism; GraphPad Software) using the Michaelis-Menten equation:

$$V = (V_{max} \times [S]) / (K_m + [S]) \quad (\text{Eq. 1})$$

where V is the rate of cholesterol esterification and [S] is the concentration of substrate. This analysis was based on the assumption that 1 mol of CE is generated per mole of UC esterified.

### Structural characterization of spherical rHDLs

Phospholipid acyl chain and head group packing order was determined as the steady-state fluorescence polarization of spherical rHDLs labeled with 1,6-diphenyl-1,3,5-hexatriene (DPH) or 1-(4-trimethylammoniumphenyl)-6-phenyl-1,3,5-hexatriene *p*-toluenesulfonate (TMA-DPH), respectively (19). As the rHDL preparations were comparable in terms of phospholipid composition, variations in the partitioning of the DPH and TMA-DPH reflect structural, rather than compositional, differences between the rHDLs. Spherical rHDLs labeled with 6-propionyl-2-(dimethylamino)-naphthalene (PRODAN) were used to assess lipid-water interfacial hydration (19). Uncorrected fluorescence emission spectra of PRODAN-labeled rHDLs were recorded from 390 to 600 nm (excitation wavelength, 366 nm) using excitation and emission band passes of 5 and 6 nm, respectively. Polarization values and emission spectra were determined at 5°C intervals from 5°C to 50°C. In all cases, the rHDL phospholipid/probe molar ratio was 500:1. The final phospholipid concentration was 0.5 mM.

### Apolipoprotein denaturation studies

Lipid-free apolipoproteins and spherical rHDLs were dialyzed against 0.01 M Tris, pH 7.4, and adjusted to 30  $\mu\text{g}/\text{ml}$  protein. The samples were incubated at 25°C for 24 h with 0–6 M guanidine hydrochloride (Gdn-HCl; MP Biomedicals, Irvine, CA). Wavelengths of maximum fluorescence were determined from 300–380 nm emission scans using an excitation wavelength of 295 nm and excitation and emission band passes of 5 and 7 nm, respectively.

Apolipoprotein unfolding was determined as the fraction unfolded:

$$(f_u) = \frac{\lambda_{\text{folded}} - \lambda}{\lambda_{\text{folded}} - \lambda_{\text{unfolded}}} \quad (\text{Eq. 2})$$

where  $\lambda_{\text{folded}}$  and  $\lambda_{\text{unfolded}}$  represent the wavelength of maximum fluorescence of the apolipoprotein in the folded and unfolded states, and  $\lambda$  is the wavelength of maximum fluorescence in the transition between the folded and unfolded states. The N- and C-terminal domains of apoE2, apoE3, and apoE4 were treated independently. The unfolding of apoA-I was regarded as a single process. The concentration of Gdn-HCl required to achieve 50% unfolding was determined from a variable-slope, sigmoidal curve (GraphPad):

$$Y = \lambda_{\text{unfolded}} + \frac{\lambda_{\text{folded}} - \lambda_{\text{unfolded}}}{1 + 10^{[(\text{Gdn-HCl})_{1/2} - X]h}} \quad (\text{Eq. 3})$$

where  $\lambda_{\text{folded}}$  and  $\lambda_{\text{unfolded}}$  are defined as above, Y is the wavelength of maximum fluorescence for a given concentration of Gdn-HCl, X is the concentration of Gdn-HCl, and h is the Hill coefficient.

### Cross-linking

ApoE2, apoE3, and apoE4 in the lipid-free form, and in spherical rHDLs, were dialyzed against 0.017 M  $\text{Na}_2\text{HPO}_4$ , 0.003 M  $\text{NaH}_2\text{PO}_4$ , 150 mM NaCl, 0.01% (w/v) EDTA- $\text{Na}_2$ , and 0.02% (w/v)  $\text{NaN}_3$ , pH 7.5 (PBS), and adjusted to 0.5 mg/ml protein. The samples (270  $\mu\text{l}$ ) were mixed with 7 mM sulfo-ethylene glycol bis[sulfosuccinimidylsuccinate] (Sulfo-EGS) (30  $\mu\text{l}$ ; Pierce Biotechnology, Rockford, IL) in PBS and incubated at 25°C for 30 min. The reaction was stopped by the addition of 1.0 mM Tris, pH 7.5 (10  $\mu\text{l}$ ). The samples were then maintained at 25°C for 15 min, dialyzed at 4°C against 0.01 M Tris, 0.001 M EDTA- $\text{Na}_2$ , and 1% (w/v) SDS, pH 8.0, incubated for 45 min at 37°C, and electrophoresed for 3 h at 150 V on a 3/40 gradient gel preequilibrated in 0.04 M Tris, 0.02 M sodium acetate, 0.002 M EDTA- $\text{Na}_2$ , and 0.2% (w/v) SDS, pH 7.4. The gels were fixed in isopropanol-acetic acid-water (25:10:65, v/v/v), stained with Coomassie Blue R-250 [0.1% (w/v) in methanol-acetic acid-water (25:10:65, v/v/v)], and destained in methanol-acetic acid-water (25:10:65, v/v/v).

### Other techniques

Electrophoresis on 3/40 nondenaturing gradient gels was used to determine rHDL size (20). Phospholipid, triglyceride (TG), and UC concentrations were determined enzymatically (21–23). A Roche Diagnostics Kit was used to determine total cholesterol concentrations. CE concentrations were calculated as the difference between total cholesterol and UC concentrations. Protein concentrations were determined by the bicinchoninic acid assay (24). All assays were carried out on a Hitachi 902 automatic analyzer (Roche Diagnostics GmbH, Mannheim, Germany). Samples for immunoblotting were electrophoresed on 3/40 nondenaturing gradient gels and transferred electrophoretically to nitrocellulose membranes. The membranes were immunoblotted with appropriate antibodies and visualized by enhanced chemiluminescence (Amersham Biosciences, Uppsala, Sweden).

### Statistical analyses

Two-way ANOVA (GraphPad) was used to determine whether differences between data sets were significant. Two-way ANOVA with Bonferroni posttests was used to compare the PRODAN data sets. In all cases, significance was set at  $P < 0.05$ .

## RESULTS

### Characterization of discoidal rHDLs

Discoidal (E2)rHDL, (E3)rHDL, (E4)rHDL, and (A-I)rHDL were prepared by the cholate dialysis method (17). The POPC/UC/apolipoprotein molar ratios of the resulting preparations ranged from 114.7:12.8:1.0 to 94.4:8.4:1.0. As judged by gel filtration chromatography, the discoidal (E2)rHDL, (E3)rHDL, and (E4)rHDL had average diameters of 17.0 nm, compared with  $\sim 10.0$  nm for the discoidal (A-I)rHDL (Fig. 1).

### Reactivity of discoidal rHDLs with LCAT

[ $^3\text{H}$ ]UC-labeled discoidal (E2)rHDL, (E3)rHDL, (E4)rHDL, and (A-I)rHDL (0.1–5.0  $\mu\text{M}$  UC) were incubated with a constant amount of LCAT. Cholesterol esterifi-

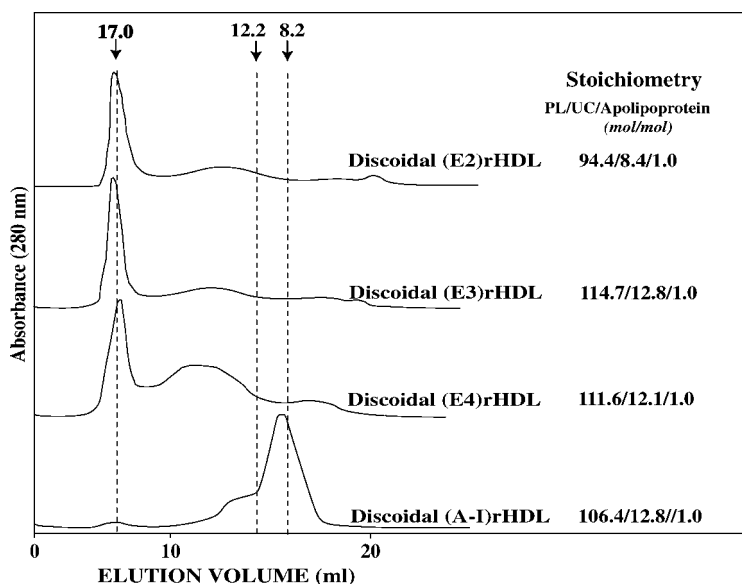


**Fig. 1.** Gel-permeation chromatography of discoidal reconstituted high density lipoprotein (rHDL) containing recombinant apolipoprotein E2 [(E2)rHDL], apoE3 [(E3)rHDL], [(E4)rHDL], and (A-I)rHDL. Discoidal (E2)rHDL (E3)rHDL, (E4)rHDL, and (A-I)rHDL were prepared by the cholate dialysis method and chromatographed on a Superose 6 column, as described in Experimental Procedures. Elution profiles for the rHDLs are shown. The elution positions of proteins of known diameter are also indicated (thyroglobulin, 17.0 nm; ferritin, 12.2 nm; and lactate dehydrogenase, 8.2 nm). PL, phospholipid; UC, unesterified cholesterol.

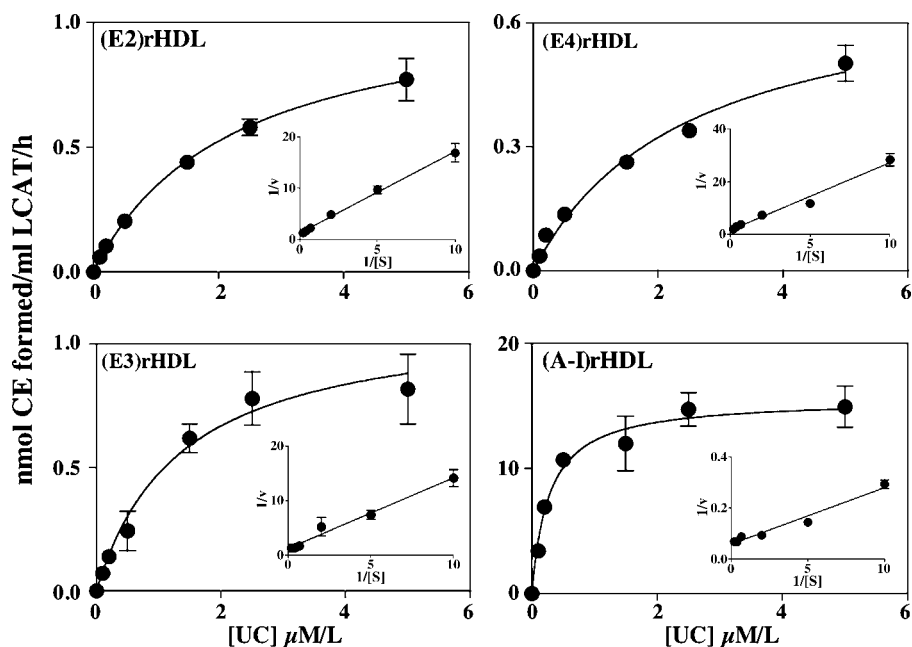


**Fig. 2.** Kinetics of LCAT-mediated cholesterol esterification in discoidal rHDLs. [ $^3\text{H}$ ]UC-labeled discoidal (E2)rHDL, (E3)rHDL, (E4)rHDL, and (A-I)rHDL (0.1–5.0  $\mu\text{M}$ /1 UC) were mixed with 1% (w/v) fatty acid-free BSA (final concentration, 3.7 mg/ml) and  $\beta$ -mercaptoethanol (final concentration, 5.0 mM). LCAT (5  $\mu\text{l}$  of a 1:5 dilution of a preparation that generated 2,144 nmol cholesteryl ester (CE)/ml LCAT/h) was added to the (A-I)rHDL. The same LCAT preparation (5.0  $\mu\text{l}$ , undiluted) was added to the (E2)rHDL, (E3)rHDL, and (E4)rHDL. In all cases, the final volume was 135  $\mu\text{l}$ . The mixtures were incubated at 37°C for 1 h. CE formation was determined as described in Experimental Procedures. Means  $\pm$  SEM of three independent experiments are shown. The insets show Lineweaver-Burk plots of the kinetic data.  $P < 0.0001$  for (A-I)rHDL versus (E2)rHDL, (E3)rHDL, and (E4)rHDL.

cation and kinetic parameters were determined as described in Experimental Procedures.  $V_{max}$  for (A-I)rHDL was  $15.92 \pm 0.91$  nmol CE formed/ml LCAT/h, compared with  $1.11 \pm 0.10$ ,  $1.12 \pm 0.14$ , and  $0.72 \pm 0.06$  nmol CE formed/ml LCAT/h for (E2)rHDL, (E3)rHDL, and

(E4)rHDL, respectively [ $P < 0.0001$  for (A-I)rHDL vs. (E2)rHDL, (E3)rHDL, and (E4)rHDL] (Fig. 2, Table 1). As judged by the  $K_m(\text{app})$  values, LCAT had a greater affinity for the discoidal (A-I)rHDL than for any of the apoE-containing rHDLs. The catalytic efficiency [ $V_{max}/K_m(\text{app})$ ] of the LCAT reaction was 50- to 150-fold greater for the discoidal (A-I)rHDL than for any of the apoE-containing rHDLs. Double reciprocal plots of the rate of cholesterol esterification versus substrate concentration were linear (Fig. 2, insets).

TABLE 1. Kinetic parameters for LCAT-mediated cholesterol esterification in discoidal rHDLs

Substrate	$V_{max}$ nM CE formed/ml LCAT/h	$K_m(\text{app})$ nM	Catalytic Efficiency $V_{max}/K_m(\text{app})$
Discoidal (E2)rHDL	$1.11 \pm 0.10$	$2.23 \pm 0.46$	0.50
Discoidal (E3)rHDL	$1.12 \pm 0.14$	$1.36 \pm 0.45$	0.82
Discoidal (E4)rHDL	$0.72 \pm 0.06^a$	$2.44 \pm 0.42$	0.29
Discoidal (A-I)rHDL	$15.92 \pm 0.91^b$	$0.30 \pm 0.06$	53.07

CE, cholesteryl ester; (E2)rHDL, reconstituted high density lipoprotein containing recombinant apolipoprotein E2; rHDL, reconstituted high density lipoprotein. Discoidal (E2)rHDL, (E3)rHDL, (E4)rHDL, and (A-I)rHDL were incubated with LCAT, as described in the legend to Fig. 2. Kinetic parameters were determined by nonlinear regression analysis of the rate of cholesterol esterification versus the concentration of substrate, as described in Experimental Procedures.

<sup>a</sup> $P < 0.0001$  for (E4)rHDL versus (E2)rHDL and (E3)rHDL.

<sup>b</sup> $P < 0.0001$  for (A-I)rHDL versus (E2)rHDL, (E3)rHDL, and (E4)rHDL.

### Physical characterization of spherical rHDLs

The discoidal (E2)rHDL, (E3)rHDL, (E4)rHDL, and (A-I)rHDL were converted into spherical rHDLs by incubation with LDL and LCAT. Most of the spherical (A-I)rHDL was 9.8 nm in diameter (Fig. 3). The spherical (E2)rHDL, (E3)rHDL, and (E4)rHDL, which were comparable to the spherical (A-I)rHDL in terms of composition, were 11.3–11.5 nm in diameter.

One explanation for the larger size of the apoE-containing spherical rHDLs is that they contained more apolipoprotein molecules per particle than the spherical (A-I)rHDL. An attempt to address this question was made by incubating the rHDLs with the bifunctional cross-linking agent bis(sulfosuccinimidyl)suberate (25, 26). These results confirmed that the spherical (A-I)rHDL contained three apoA-I molecules per particle (data not shown)



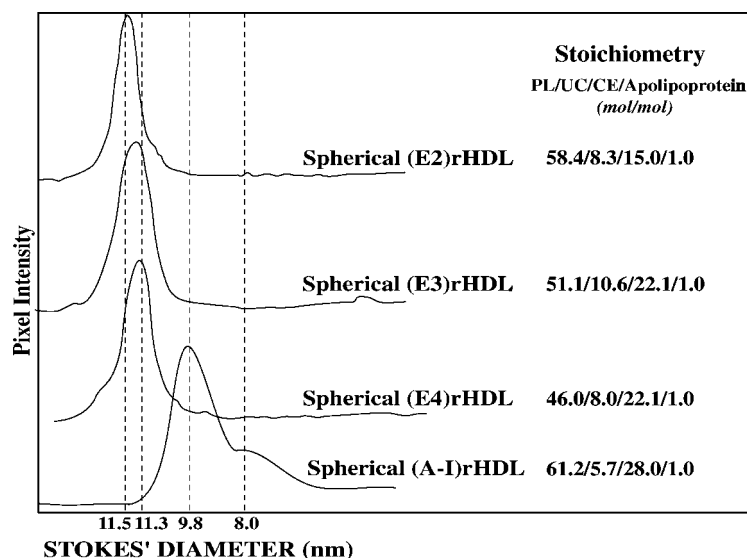


**Fig. 3.** Physical properties of spherical rHDLs. Discoidal (E2)rHDL, (E3)rHDL, (E4)rHDL, and (A-I)rHDL were incubated at 37°C for 24 h with LDL and LCAT. The resulting spherical rHDLs were isolated by ultracentrifugation, electrophoresed on a nondenaturing 3/40 polyacrylamide gradient gel, stained with Coomassie Blue, and scanned with a laser densitometer. Particle diameters were determined by reference to high molecular weight standards. Stoichiometries were calculated from triplicate determinations of the concentrations of individual constituents. PL, phospholipid.

(25, 26). The apolipoproteins in the spherical (E2)rHDL, (E3)rHDL, and (E4)rHDL were not cross-linked by bis(sulfosuccinimidyl)suberate (data not shown). This problem was circumvented by incubating the spherical (E2)rHDL, (E3)rHDL, and (E4)rHDL, as well as lipid-free apoE2, apoE3, and apoE4, with Sulfo-EGS, a cross-linker that has a longer spacer arm than bis(sulfosuccinimidyl)suberate. When these samples were subjected to SDS-PAGE, dimers, trimers, and tetramers were apparent in the lipid-free apoE2 and apoE3 incubations (**Fig. 4**). Only dimers and trimers were generated in the incubation that contained lipid-free apoE4. The cross-linked spherical (E2)rHDL, (E3)rHDL,

and (E4)rHDL comigrated with trimeric, lipid-free apoE, indicating that these preparations all contained three apoE molecules per particle. This result indicates that the difference in size between the spherical, apoE-containing rHDLs and the spherical (A-I)rHDL may reflect the strikingly different abilities of the apolipoproteins to limit the curvature of a lipid-water interface. As was the case with lipid-free apoE4, the spherical (E4)rHDL was cross-linked less efficiently than either the spherical (E2)rHDL or the spherical (E3)rHDL.

#### Structural characterization of spherical rHDLs

Phospholipid acyl chain and head group packing order was assessed as the steady-state fluorescence polarization of rHDL labeled with DPH and TMA-DPH, respectively (**Fig. 5**). The polarization of the DPH-labeled spherical (A-I)rHDL (closed circles) was decreased relative to spherical (E2)rHDL (closed triangles), spherical (E3)rHDL (closed squares), and spherical (E4)rHDL (open circles) [ $P < 0.0001$  for (A-I)rHDL vs. (E2)rHDL, (E3)rHDL, and (E4)rHDL]. This indicates that the phospholipid acyl chains in spherical (A-I)rHDL are less ordered than those in apoE-containing rHDLs.

The polarization studies also established that apoE isoforms regulate spherical rHDL phospholipid acyl chain and head group packing order. Both the acyl chains and head groups in the (E3)rHDL were less ordered than in either the (E2)rHDL or the (E4)rHDL [ $P < 0.0001$  for (E2)rHDL vs. (E3)rHDL and (E4)rHDL and for (E3)rHDL vs. (E4)rHDL for the DPH-labeled rHDL;  $P < 0.0001$  for (E3)rHDL vs. (E2)rHDL and (E4)rHDL for the TMA-DPH-labeled rHDL]. This is consistent with what has been reported previously (16). The (A-I)rHDL (data not shown), (E2)rHDL, and (E4)rHDL TMA-DPH polarization values were comparable.

The wavelengths of maximum fluorescence of the PRODAN-labeled rHDL were comparable at 5–10°C. From 10°C to 35°C, the surface hydration of the (E2)rHDL (closed triangles), (E4)rHDL (open circles), and (A-I)rHDL (closed

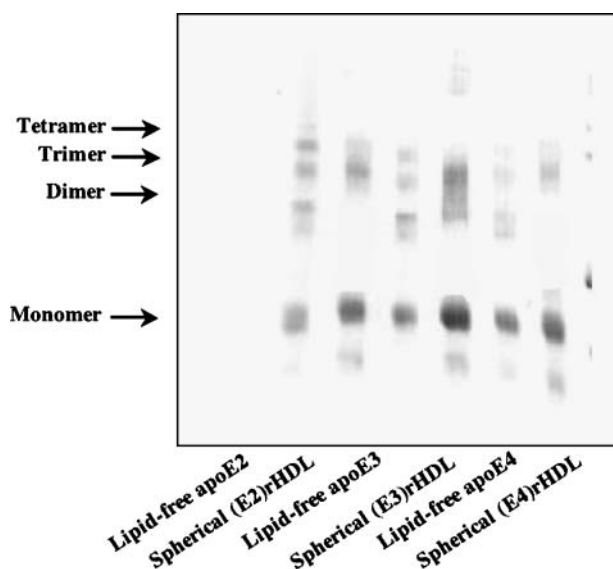


**Fig. 4.** Cross-linking of apoE2, apoE3, and apoE4 in the lipid-free form and in spherical rHDLs. Lipid-free and lipid-associated apoE2, apoE3, and apoE4 were cross-linked with sulfo-ethylene glycol bis[sulfosuccinimidylsuccinate] and subjected to SDS-polyacrylamide gradient gel electrophoresis, as described in Experimental Procedures. A scan of the Coomassie Blue-stained gradient gel is shown.

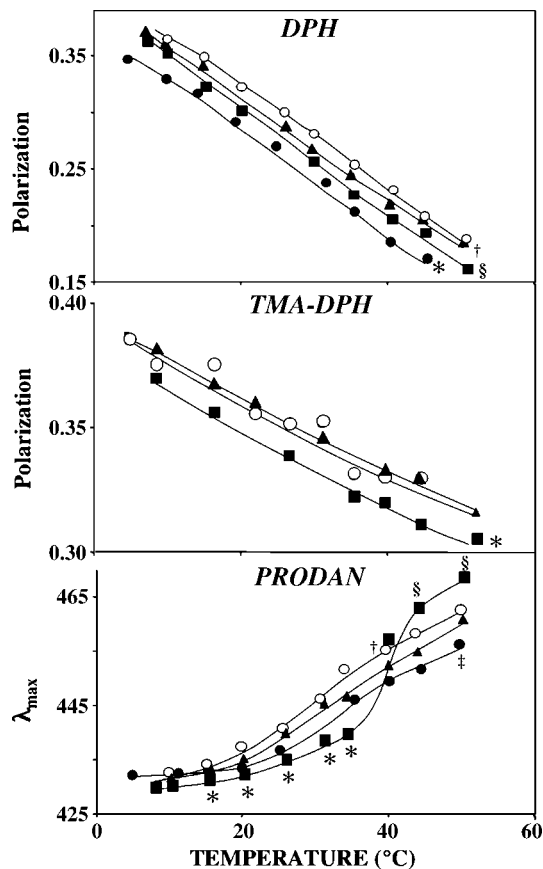


**Fig. 5.** Structural properties of spherical rHDLs. Spherical (E2)rHDL (closed triangles), (E3)rHDL (closed squares), (E4)rHDL (open circles), and (A-I)rHDL (closed circles) were labeled with 1,6-diphenyl-1,3,5-hexatriene (DPH), 1-(4-trimethylammoniumphenyl)-6-phenyl-1,3,5-hexatriene *p*-toluenesulfonate (TMA-DPH), or 6-propionyl-2-(dimethylamino)-naphthalene (PRODAN). Steady-state fluorescence polarization of the DPH- and TMA-DPH-labeled samples, and the wavelength of maximum fluorescence of the PRODAN-labeled samples, were determined as a function of temperature. All values represent means  $\pm$  SEM of at least three determinations. For DPH, \*  $P < 0.0001$  for (A-I)rHDL versus (E2)rHDL, (E3)rHDL, and (E4)rHDL; †  $P < 0.0001$  for (E2)rHDL versus (E3)rHDL and (E4)rHDL; §  $P < 0.0001$  for (E3)rHDL versus (E4)rHDL. For TMA-DPH, \*  $P < 0.0001$  for (E3)rHDL versus (E2)rHDL and (E4)rHDL. For PRODAN, \*  $P < 0.0001$  for (E3)rHDL versus (E2)rHDL, (E4)rHDL, and (A-I)rHDL; †  $P < 0.001$  for (E3)rHDL versus (A-I)rHDL; §  $P < 0.0005$  for (E3)rHDL versus (E2)rHDL and (E4)rHDL; ‡  $P < 0.0001$  for (E3)rHDL versus (A-I)rHDL.

circles) increased more rapidly than that of the (E3)rHDL (closed squares) [ $P < 0.0001$  for (E3)rHDL vs. (E2)rHDL, (E4)rHDL, and (A-I)rHDL]. At temperatures of  $>40^{\circ}\text{C}$ , the (E3)rHDL lipid-water interfacial hydration was enhanced relative to that of the other rHDLs [ $P < 0.0005$  for (E3)rHDL vs. (E2)rHDL and (E4)rHDL;  $P < 0.0001$  for (E3)rHDL vs. (A-I)rHDL].

#### Denaturation of apoE2, apoE3, apoE4, and apoA-I in the lipid-free form and in spherical rHDLs

When full-length lipid-free apoE2 (Fig. 6A, closed circles), apoE3 (Fig. 6B, closed circles), and apoE4 (Fig. 6C, closed circles) were incubated with Gdn-HCl, their N- and

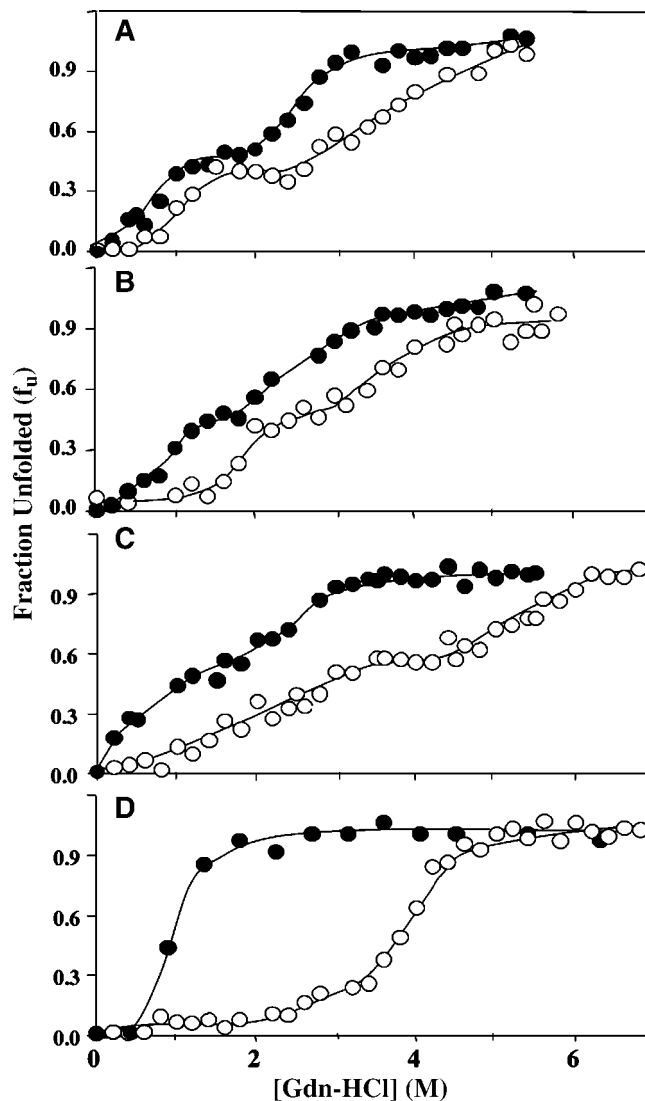


**Fig. 6.** Unfolding of apoE2, apoE3, apoE4, and apoA-I in the lipid-free form and in spherical rHDLs. Lipid-free apoE2 (A, closed circles), apoE3 (B, closed circles), apoE4 (C, closed circles), and apoA-I (D, closed circles) and spherical (E2)rHDL (A, open circles), (E3)rHDL (B, open circles), (E4)rHDL (C, open circles), and (A-I)rHDL (D, open circles) were incubated at  $25^{\circ}\text{C}$  for 24 h with 0.0–6.0 M Gdn-HCl. The fractional unfolding of the apolipoproteins ( $f_u$ ) at each Gdn-HCl concentration was determined as described in Experimental Procedures.

C-terminal domains unfolded independently. This is consistent with what has been reported elsewhere (27). The midpoints for the unfolding of the C- and N-terminal domains of apoE2 were  $0.80 \pm 0.09$  and  $2.45 \pm 0.09$  M Gdn-HCl, respectively (Table 2), with a plateau at 1.5 M Gdn-HCl. For lipid-free apoE3, the respective midpoints of unfolding of the C- and N-terminal domains were  $0.84 \pm 0.07$  and  $2.34 \pm 0.28$  M Gdn-HCl. A plateau, which was less pronounced than for lipid-free apoE2, was apparent at 1.6 M Gdn-HCl. In the case of lipid-free apoE4, the C- and N-terminal domains unfolded in a noncooperative manner, with a shoulder, rather than a distinct plateau, at 2.2–2.4 M Gdn-HCl. As the unfolding of the C- and

TABLE 2. Unfolding of apoE2, apoE3, and apoE4 in the lipid-free form and in spherical rHDLs

Lipid-Free ApoE2		Lipid-Free ApoE3		Lipid-Free ApoE4	
C-Terminal Domain	N-Terminal Domain	C-Terminal Domain	N-Terminal Domain	C-Terminal Domain	N-Terminal Domain
$[Gdn-HCl]_{1/2}$ (M)		$[Gdn-HCl]_{1/2}$		$[Gdn-HCl]_{1/2}$	
0.80 ± 0.09	2.45 ± 0.09	0.84 ± 0.07	2.34 ± 0.28	n.d.	n.d.
Spherical (E2)rHDL		Spherical (E3)rHDL		Spherical (E4)rHDL	
C-Terminal Domain	N-Terminal Domain	C-Terminal Domain	N-Terminal Domain	C-Terminal Domain	N-Terminal Domain
$[Gdn-HCl]_{1/2}$ (M)		$[Gdn-HCl]_{1/2}$		$[Gdn-HCl]_{1/2}$	
1.03 ± 0.19	3.39 ± 0.54	1.85 ± 0.13	3.89 ± 0.18	2.00 ± 0.21	5.44 ± 0.10

ApoE2, apoE3, and apoE4 in the lipid-free form and in spherical rHDLs were incubated at 25°C for 24 h with 0.0–6.0 M Gdn-HCl.  $[Gdn-HCl]_{1/2}$  values (the concentration of Gdn-HCl required to achieve 50% unfolding of apoE) were calculated as described in Experimental Procedures. All values represent means ± SEM (n ≥ 3). n.d., not determined.

N-terminal domains of apoE4 overlapped, the midpoints of unfolding were not determined. The unfolding of lipid-free apoA-I (Fig. 6D, closed circles) was monophasic and essentially complete at 1.5 M Gdn-HCl. This is consistent with what has been reported previously (11).

Higher concentrations of Gdn-HCl were required to unfold the apolipoproteins when they were incorporated into spherical rHDLs (Fig. 6, open circles). The midpoints for the unfolding of the two domains of lipid-associated apoE2 were 1.03 ± 0.19 and 3.39 ± 0.54 M Gdn-HCl (Fig. 6A), compared with 1.85 ± 0.13 and 3.89 ± 0.18 M Gdn-HCl for lipid-associated apoE3 (Fig. 6B, Table 2). The midpoints for the unfolding of the two domains of lipid-associated apoE4 were 2.00 ± 0.21 and 5.44 ± 0.10 M Gdn-HCl, with a distinct plateau at 3.8 M Gdn-HCl (Fig. 6C). The midpoint of unfolding of lipid-associated apoA-I was 3.7 ± 0.1 M Gdn-HCl (Fig. 6D).

### Remodeling of spherical rHDLs by CETP

Previous studies from this laboratory have established that incubation with CETP and Intralipid® remodels spherical (A-I)rHDL into small, core lipid-depleted particles in a process that generates lipid-free or lipid-poor apoA-I (26).

To determine whether this was also the case for spherical (E2)rHDL, (E3)rHDL, and (E4)rHDL, incubations were carried out with Intralipid® in the presence and absence of CETP. Incubation with Intralipid® alone did not alter the composition of the (E2)rHDL, (E3)rHDL, or (E4)rHDL (Table 3). The small amount of TG in these samples probably reflects a minor carryover of Intralipid® into the rHDL fraction rather than a spontaneous transfer of TG from Intralipid® to the rHDL (26). When CETP was included in the incubations, the rHDLs were all progressively depleted of CE and enriched with TG. The phospholipid-apolipoprotein molar ratio of the spherical (A-I)rHDL, but not the spherical (E2)rHDL, (E3)rHDL, or (E4)rHDL, also increased. Immunoblot analysis of the spherical (A-I)rHDL incubation mixtures established that the increased phospholipid/apoA-I molar ratio was attributable to dissociation of apoA-I from the particles (data not shown). This is consistent with what has been reported previously (26). Immunoblot analysis of the (E2)rHDL, (E3)rHDL, and (E4)rHDL incubation mixtures

established that CETP did not mediate the dissociation of apoE (data not shown).

There were also major differences between the apoE-containing rHDLs and the (A-I)rHDL in terms of particle remodeling (Fig. 7). Whereas incubation with CETP and Intralipid® converted most of the spherical (A-I)rHDL into small particles (diameter, 8.0 nm), the spherical (E2)rHDL, (E3)rHDL, and (E4)rHDL increased in size. To determine whether this observation could be explained in terms of core lipid transfers, the molar ratios of CE/apolipoprotein (closed circles), TG/apolipoprotein (open circles), and total core lipids, CE + TG/apolipoprotein (closed triangles), were plotted as a function of incubation time (Fig. 8). This established that all of the rHDLs were depleted of core lipids to the same extent. Therefore, it was concluded that the increase in (E2)rHDL, (E3)rHDL, and (E4)rHDL size could not be explained in terms of core lipid transfers.

This raised the possibility that incubation with CETP may have mediated the fusion of the apoE-containing spherical rHDLs to generate large conversion products that contained six molecules of apoE per particle. To determine whether this was the case, an unsuccessful attempt was made to cross-link the large conversion products with Sulfo-EGS. It should be noted that, even if this approach had succeeded, the results would have been equivocal because lipid-free apoE, which is used as a standard in these experiments, does not cross-link beyond a tetramer (Fig. 4).

Therefore, an alternative strategy was used to determine whether particle fusion was responsible for the increase in (E2)rHDL, (E3)rHDL, and (E4)rHDL size. The Stokes' diameters in Fig. 7 were used to calculate the surface areas of the rHDLs that had been incubated for 24 h in the presence and absence of CETP. The stoichiometries in Table 3 were then used to calculate the total area occupied by the individual constituents on the surface of these particles. These calculations were based on three assumptions: *i*) the large, apoE-containing rHDLs are fusion products with six apoE molecules per particle; *ii*) the average area of each amino acid residue is 0.15 nm<sup>2</sup> (28); and *iii*) after taking into account movement within the lateral plane of the lipoprotein surface as well as surface irregu-

TABLE 3. Composition of spherical rHDLs after incubation with CETP and Intralipid®

Spherical rHDL	Additions	Incubation Conditions	Stoichiometry				Protein
			PL	UC	CE	TG	
					<i>mol/mol</i>		
(E2)rHDL	Intralipid®, - CETP	4°C, 24 h	63.0	12.2	23.9	2.3	1.0
	Intralipid®, - CETP	37°C, 24 h	79.2	3.3	34.6	2.8	1.0
	Intralipid®, + CETP	37°C, 1 h	66.4	16.6	18.3	7.2	1.0
	Intralipid®, + CETP	37°C, 3 h	71.5	16.0	14.1	14.5	1.0
	Intralipid®, + CETP	37°C, 6 h	63.5	11.6	5.9	19.4	1.0
	Intralipid®, + CETP	37°C, 12 h	62.5	8.1	2.6	21.0	1.0
	Intralipid®, + CETP	37°C, 24 h	53.6	5.2	0.6	15.9	1.0
(E3)rHDL	Intralipid®, - CETP	4°C, 24 h	58.0	12.2	25.6	3.7	1.0
	Intralipid®, - CETP	37°C, 24 h	57.5	6.1	24.4	4.0	1.0
	Intralipid®, + CETP	37°C, 1 h	67.8	16.3	24.4	14.1	1.0
	Intralipid®, + CETP	37°C, 3 h	51.5	11.1	11.5	13.8	1.0
	Intralipid®, + CETP	37°C, 6 h	52.1	9.3	6.0	18.1	1.0
	Intralipid®, + CETP	37°C, 12 h	51.9	6.0	1.8	17.3	1.0
	Intralipid®, + CETP	37°C, 24 h	44.1	4.2	0.2	14.1	1.0
(E4)rHDL	Intralipid®, - CETP	4°C, 24 h	48.2	7.1	25.0	3.3	1.0
	Intralipid®, - CETP	37°C, 24 h	54.3	2.9	27.5	3.6	1.0
	Intralipid®, + CETP	37°C, 1 h	47.0	9.7	16.8	12.4	1.0
	Intralipid®, + CETP	37°C, 3 h	49.3	6.9	4.5	24.3	1.0
	Intralipid®, + CETP	37°C, 6 h	43.4	8.2	10.8	14.2	1.0
	Intralipid®, + CETP	37°C, 12 h	44.0	4.5	0.3	20.7	1.0
	Intralipid®, + CETP	37°C, 24 h	53.3	3.5	0.7	20.2	1.0
(A-I)rHDL	Intralipid®, - CETP	4°C, 24 h	56.1	3.0	24.8	4.7	1.0
	Intralipid®, - CETP	37°C, 24 h	56.8	1.4	24.0	4.3	1.0
	Intralipid®, + CETP	37°C, 1 h	53.5	5.0	11.9	8.8	1.0
	Intralipid®, + CETP	37°C, 3 h	67.1	3.6	3.6	12.8	1.0
	Intralipid®, + CETP	37°C, 6 h	73.3	2.6	3.2	10.9	1.0
	Intralipid®, + CETP	37°C, 12 h	81.1	2.0	0.5	10.0	1.0
	Intralipid®, + CETP	37°C, 24 h	77.3	1.6	0.5	8.5	1.0

CETP, cholesteryl ester transfer protein; PL, phospholipid; TG, triglyceride; UC, unesterified cholesterol. Spherical (E2)rHDL, (E3)rHDL, (E4)rHDL, and (A-I)rHDL were mixed with Intralipid® and incubated for 0–24 h in the presence or absence of CETP. The final rHDL CE and Intralipid® TG concentrations were 0.1 and 4.0 mM/l, respectively. The samples without CETP were either maintained at 4°C or incubated at 37°C for 24 h. The samples that contained CETP (final activity, 2.7 U/ml) were incubated at 37°C for 1, 3, 6, 12, or 24 h. The final volume of the incubation mixtures was 2.0 ml. After incubation, the rHDLs were isolated by ultracentrifugation ( $1.07 < d < 1.21$  g/ml) and their composition was determined as described in Experimental Procedures. All concentrations were measured in triplicate. The values varied by <10%.

larities, the average solvent-accessible surface area of a phospholipid molecule is  $1.27 \text{ nm}^2$  (29). The “observed” surface areas that were determined from the Stokes’ diameters were then compared with the “calculated” values obtained from the stoichiometries. The results are presented in **Table 4**.

This approach was validated for spherical (A-I)rHDL, for which cross-linking has been used to establish that the decrease in particle size that occurs during incubation with CETP and Intralipid® is accompanied by a reduction in the number of apoA-I molecules from three to two per particle (26). As there was close agreement between the two approaches for all of the rHDLs, it was concluded that particle fusion is the most likely explanation for the increase in spherical (E2)rHDL, (E3)rHDL, and (E4)rHDL size.

## DISCUSSION

Approximately 75% of the apoE in normolipidemic plasma is associated with spherical HDLs that are 9.0–18.5 nm in diameter and do not contain apoA-I (2–5). Despite the fact that such particles account for as much as 10% of the total HDL fraction, remarkably little is known about their origin, structure, and metabolism. These issues have

been addressed in this report, which shows for the first time that *i*) LCAT converts discoidal (E2)rHDL, (E3)rHDL, and (E4)rHDL into intermediate-sized spherical rHDLs (diameter, 11.3–11.5 nm), which are structurally distinct from each other as well as from spherical (A-I)rHDL, and *ii*) CETP remodels these intermediate-sized apoE-containing spherical rHDLs into large fusion products (diameter, 13.2–15.1 nm) without mediating the dissociation of apoE.

The results also show that apoE activates LCAT less effectively than apoA-I. This is in agreement with an earlier study, which established that LCAT has a lower affinity for discoidal rHDLs that contain apoE of unknown genotype than for discoidal (A-I)rHDL (30). The results of that study also established that the rate of cholesterol esterification in discoidal (A-I)rHDL was approximately double that in apoE-containing discoidal rHDLs. Although the same general trends were observed in this report, we found that cholesterol was esterified 15–20 times more rapidly in the discoidal (A-I)rHDL than in the apoE-containing discoidal rHDLs (Table 1). This discrepancy may be related to the different phospholipid contents of the discoidal rHDLs. Although the discs in the current study contained POPC, the discs in the earlier report were prepared with egg phosphatidylcholine, which comprises a mixture of phospholi-



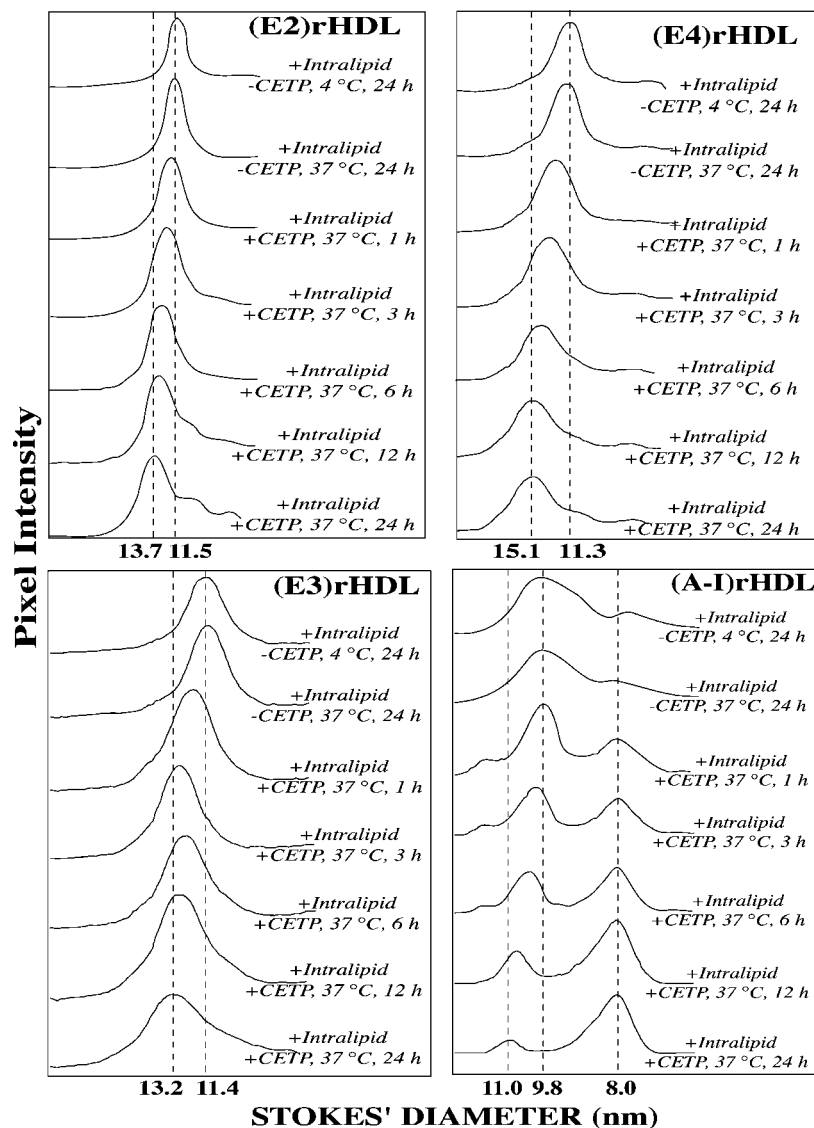


**Fig. 7.** Remodeling of spherical rHDLs by CETP and Intralipid®: changes in particle size. Spherical (E2)rHDL, (E3)rHDL, (E4)rHDL, and (A-I)rHDL were mixed with Intralipid® and incubated in the presence or absence of CETP, as described in the legend to Table 3. When the incubations were complete, the rHDLs were isolated by ultracentrifugation and electrophoresed on nondenaturing polyacrylamide gradient gels. Laser densitometric scans of Coomassie Blue-stained gels are shown.

pids with acyl chains of varying length and unsaturation that do not access the active site of LCAT equally well (31, 32). It should also be noted that the kinetic parameters in this study were derived by nonlinear regression analysis, whereas the values in the earlier study were calculated manually from Lineweaver-Burk plots.

The results presented here also established that the isoforms of apoE do not all activate LCAT equally well. The possibility that these results are a reflection of variations in the size of the discoidal, apoE-containing rHDLs is excluded by the results in Fig. 1. Therefore, the lower  $V_{max}$  and catalytic efficiency for the discoidal (E4)rHDL, relative to the discoidal (E2)rHDL and (E3)rHDL, may be a reflection of the discoidal (E4)rHDL phospholipid acyl chains not being able to access the active site of LCAT as readily as the less ordered acyl chains in the discoidal (E2)rHDL and (E3)rHDL (Fig. 5). This is also consistent with an earlier report showing that the activation energy of the LCAT reaction increases as the substrate phospholipid acyl chains become more ordered and motionally restricted (32).

The finding that the phospholipid head groups and acyl chains in spherical (E3)rHDL are less ordered than in either (E2)rHDL or (E4)rHDL is also noteworthy. This is most likely caused by the reduced surface hydration of the spherical (E3)rHDL, enabling the apoE3  $\alpha$ -helical regions to penetrate farther into the rHDL surface. The additional finding that the phospholipid acyl chains in apoE-containing spherical rHDLs are more ordered than in spherical (A-I)rHDL probably reflects the reduced surface curvature of the larger apoE-containing rHDLs. This is consistent with NMR data, which show that phospholipid acyl chain packing order increases with decreasing lipid-water interfacial curvature (33).

Previous work from this and other laboratories have shown that association with lipid enhances the stability of apoA-I (11, 34). Our results establish that this is also the case for apoE (Fig. 6, Table 2). It is noteworthy that association with lipid markedly increased the cooperativity of the unfolding of the domains of apoE4. Although the underlying reason for this increase is not entirely clear, it

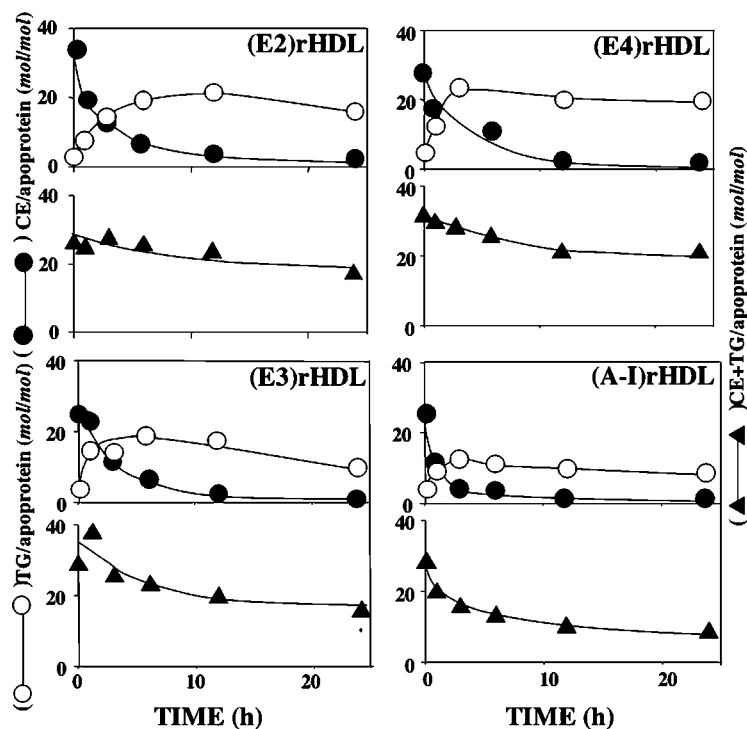


**Fig. 8.** Remodeling of spherical rHDLs by CETP and Intralipid®: core lipid transfers. Spherical (E2)rHDL, (E3)rHDL, (E4)rHDL, and (A-I)rHDL were incubated with CETP and Intralipid®, as described in the legend to Table 3. CE/apolipoprotein (closed circles), triglyceride (TG)/apolipoprotein (open circles), and CE + TG/apolipoprotein (closed triangles) molar ratios are shown.

suggests that association with lipid may alter the molten globule structure, and possibly the domain interactions, of apoE4. This finding has obvious implications for the role of apoE4 in neurodegeneration, in which the molten globule is involved in a number of key processes, such as amyloid fibril formation and the development of Alzheimer's disease (35, 36).

The results presented in this report may also be relevant to cholesterol transport in the central nervous system, where apoE-containing rHDLs, rather than (A-I)rHDL, are important for regulating cholesterol transport. In the brain, apoE is secreted as a component of discoidal rHDLs from astrocytes and microglia (37, 38). As is the case in

plasma, these discs are most likely converted by LCAT into spherical particles that play a key role in maintaining cholesterol homeostasis in the brain.

One of the most unexpected observations to emerge from this study is that apoE-containing spherical rHDLs increase in size when they interact with CETP. Although this observation appears to be at odds with the presence of large, apoE-containing rHDLs in the plasma of subjects who are deficient in CETP or in whom the activity of CETP is pharmacologically inhibited, it is important to note that the large rHDLs in those individuals are generated as a consequence of CE accumulating in the particle core (39, 40). By contrast, the large apoE-containing rHDLs in this

**TABLE 4.** Effects of CETP remodeling on the number of apolipoprotein molecules per rHDL particle

Spherical rHDL	Incubation Conditions	Additions	Apolipoprotein Molecules/Particle	rHDL Surface Area	
				Observed <sup>a</sup>	Calculated <sup>b</sup>
				<i>nm</i> <sup>2</sup>	
(E2)rHDL	37°C, 24 h	Intralipid®, -CETP	3 <sup>c</sup>	415.5	436.4
	37°C, 24 h	Intralipid®, +CETP	6	589.6	677.5
(E3)rHDL	37°C, 24 h	Intralipid®, -CETP	3 <sup>c</sup>	408.3	353.7
	37°C, 24 h	Intralipid®, +CETP	6	547.4	605.1
(E4)rHDL	37°C, 24 h	Intralipid®, -CETP	3 <sup>c</sup>	401.1	341.5
	37°C, 24 h	Intralipid®, +CETP	6	716.3	675.2
(A-I)rHDL	37°C, 24 h	Intralipid®, -CETP	3 <sup>c</sup>	301.7	325.8
	37°C, 24 h	Intralipid®, +CETP	2 <sup>c</sup>	201.1	269.2

Observed surface areas for spherical (E2)rHDL, (E3)rHDL, (E4)rHDL, and (A-I)rHDL were determined from the Stokes' diameters in Fig. 7. The stoichiometries in Table 3 were used to determine calculated surface areas, assuming that incubation of spherical (E2)rHDL, (E3)rHDL, and (E4)rHDL with CETP and Intralipid® generates a fusion product with six apoE molecules per particle. Cross-linking with bis(sulfosuccinimidyl)suberate has established that the number of apoA-I molecules in spherical (A-I)rHDL decreases from three to two per particle during incubation with CETP and Intralipid® (26).

<sup>a</sup> Calculated from Stokes' diameters.


<sup>b</sup> Calculated from particle stoichiometries, assuming surface areas of 1.27 nm<sup>2</sup>/phospholipid molecule and 0.15 nm<sup>2</sup>/amino acid residue.

<sup>c</sup> Determined by cross-linking.

study were generated by a process that involved core lipid depletion and particle fusion.

The finding that the CETP-mediated remodeling of apoE-containing spherical rHDLs is distinct from what has been reported for spherical (A-I)rHDL indicates that apolipoproteins play a key role in HDL-CETP interactions. It is well established that CETP is able to deplete rHDLs of core lipids and generate destabilized particles that have an excess of surface constituents. In the case of (A-I)rHDL, this destabilization is alleviated by the dissociation of lipid-free or lipid-poor apoA-I and a reduction in particle size. The apoE-containing rHDLs, by contrast, undergo fusion to generate large particles in a process that does not involve the dissociation of apoE. The inability of apoE to dissociate from rHDLs most likely reflects the high affinity of its C-terminal domain for lipid. It also raises the possibility that closure of the four helix bundle in the N-terminal domain, which would occur if apoE were to dissociate from the rHDLs, may be energetically unfavorable. Alternatively, the N-terminal domain may "dissociate" from the rHDL surface and adopt a highly stable helix bundle, whereas the C-terminal domain remains firmly anchored to the particle surface (41).

Irrespective of why apoE does not dissociate from rHDLs, this result raises the possibility that the apoE that partitions from HDL to TG-rich lipoproteins in the postprandial state, and back to HDL in the fasted state, may be lipid-associated. As the phospholipid content of TG-rich lipoproteins varies according to dietary fat intake (42), it follows that the cycling of apoE between TG-rich lipoproteins and HDL may significantly affect HDL phospholipid composition. When this possibility is considered in light of earlier work from this laboratory, which shows that phospholipids regulate the CETP-mediated remodeling of HDL (43), it follows that apoE has the potential to affect HDL remodeling and subpopulation distribution at multiple levels.

In conclusion, this study provides the first insight into how apoE isoforms affect HDL structure, function, and remodeling. It also elucidates the pathways that are involved in the formation of apoE-containing HDLs of varying size. It is proposed in future studies to investigate how apoE and its isoforms affect the antiinflammatory and antiatherogenic properties of HDL. 

K-A.R. is a Principal Career Research Fellow of the National Heart Foundation of Australia. This research was supported by the National Health and Medical Research Council of Australia (Grant 222722).

## REFERENCES

- Cheung, M. C., and J. J. Albers. 1984. Characterization of lipoprotein particles isolated by immunoaffinity chromatography. Particles containing A-I and A-II and particles containing A-I but no A-II. *J. Biol. Chem.* **259**: 12201–12209.
- Krimbou, L., M. Tremblay, J. Davignon, and J. S. Cohn. 1997. Characterization of human plasma apolipoprotein E-containing lipoproteins in the high density lipoprotein size range: focus on pre-beta1-LpE, pre-beta2-LpE, and alpha-LpE. *J. Lipid Res.* **38**: 35–48.
- Krimbou, L., M. Marcil, H. Chiba, and J. Genest, Jr. 2003. Structural and functional properties of human plasma high density-sized lipoprotein containing only apoE particles. *J. Lipid Res.* **44**: 884–892.
- Asztalos, B. F., K. V. Horvath, K. Kajinami, C. Nartsupha, C. E. Cox, M. Batista, E. J. Schaefer, A. Inazu, and H. Mabuchi. 2004. Apolipoprotein composition of HDL in cholesteryl ester transfer protein deficiency. *J. Lipid Res.* **45**: 448–455.
- Mackie, A., M. J. Caslake, C. J. Packard, and J. Shepherd. 1981. Concentration and distribution of human plasma apolipoprotein E. *Clin. Chim. Acta.* **116**: 35–45.
- Mahley, R. W. 1988. Apolipoprotein E: cholesterol transport protein with expanding role in cell biology. *Science.* **240**: 622–630.
- Weisgraber, K. H., S. C. Rall, and R. W. Mahley. 1981. Human E apoprotein heterogeneity. Cysteine-arginine interchanges in the amino acid sequence of the apo-E isoforms. *J. Biol. Chem.* **256**: 9077–9083.
- Rall, S. C., K. H. Weisgraber, and R. W. Mahley. 1982. Human apolipoprotein E. The complete amino acid sequence. *J. Biol. Chem.* **257**: 4171–4178.
- Mitchell, C. D., W. C. King, K. R. Applegate, T. Forte, J. A. Glomset, K. R. Norum, and E. Gjone. 1980. Characterization of apolipoprotein E-rich high density lipoproteins in familial lecithin:cholesterol acyltransferase deficiency. *J. Lipid Res.* **21**: 625–634.
- Böttcher, A., J. Schlosser, F. Kronenberg, H. Dieplinger, G. Knipping, K. J. Lackner, and G. Schmitz. 2000. Preparative free-solution isotachopheresis for separation of human plasma lipoproteins: apolipoprotein and lipid composition of HDL subfractions. *J. Lipid Res.* **41**: 905–915.
- Rye, K-A., N. J. Hime, and P. J. Barter. 1996. The influence of sphingomyelin on the structure and function of reconstituted high density lipoproteins. *J. Biol. Chem.* **271**: 4243–4250.
- Piran, U., and R. J. Morin. 1979. A rapid radioassay procedure for plasma lecithin-cholesterol acyltransferase. *J. Lipid Res.* **20**: 1040–1043.
- Burstein, M., H. R. Scholnick, and R. Morfin. 1970. Rapid method for the isolation of lipoproteins from human serum by precipitation with polyanions. *J. Lipid Res.* **11**: 583–595.
- Tollefson, J. H., A. Lui, and J. J. Albers. 1988. Regulation of plasma lipid transfer by the high-density lipoproteins. *Am. J. Physiol.* **255**: E894–E902.
- Morrow, J. A., K. S. Arnold, and K. H. Weisgraber. 1999. Functional characterization of apolipoprotein E isoforms overexpressed in *Escherichia coli*. *Protein Expr. Purif.* **16**: 224–230.
- Hime, N. J., K. J. Drew, C. Hahn, P. J. Barter, and K-A. Rye. 2004. Apolipoprotein E enhances hepatic lipase-mediated hydrolysis of reconstituted high-density lipoprotein phospholipid and triacylglycerol in an isoform-dependent manner. *Biochemistry.* **43**: 12306–12314.
- Matz, C. E., and A. Jonas. 1982. Micellar complexes of human apolipoprotein A-I with phosphatidylcholines and cholesterol prepared from cholate-lipid dispersions. *J. Biol. Chem.* **257**: 4535–4540.
- Jonas, A., K. E. Kézdy, M. I. Williams, and K-A. Rye. 1988. Lipid transfers between reconstituted high density lipoprotein complexes and low density lipoproteins: effects of plasma protein factors. *J. Lipid Res.* **29**: 1349–1357.
- Rye, K-A., and P. J. Barter. 1994. The influence of apolipoproteins on the structure and function of spheroidal, reconstituted high density lipoproteins. *J. Biol. Chem.* **269**: 10298–10303.
- Rainwater, D. L., D. W. Andres, A. L. Ford, W. F. Lowe, P. J. Blanche, and R. M. Krauss. 1992. Production of polyacrylamide gradient gels for the electrophoretic resolution of lipoproteins. *J. Lipid Res.* **33**: 1876–1881.
- Takayama, M., S. Itoh, T. Nagasaki, and I. Tanimizu. 1977. A new enzymatic method for determination of serum choline-containing phospholipids. *Clin. Chim. Acta.* **79**: 93–98.
- Wahlefeld, A. W. 1974. *Methods of Enzymatic Analysis*. 2<sup>nd</sup> edition. H. U. Bergmeyer, editor. Academic Press, New York. 1831–1835.
- Stahler, F., W. Gruber, K. Stinshoff, and P. Roschlau. 1977. A practical enzymatic cholesterol determination. *Med. Lab. (Stuttg.)* **30**: 29–37.
- Smith, P. K., R. I. Krohn, G. T. Hermanson, A. K. Mallia, F. H. Gartner, M. D. Provenzano, E. K. Fujimoto, N. M. Goeke, B. J. Olson, and D. C. Klenk. 1985. Measurement of protein using bicinchoninic acid. *Anal. Biochem.* **150**: 76–85.
- Rye, K-A., and N. M. Duong. 2000. Influence of phospholipid depletion on the size, structure, and remodeling of reconstituted high density lipoproteins. *J. Lipid Res.* **41**: 1640–1650.

26. Rye, K-A., N. J. Hime, and P. J. Barter. 1995. The influence of cholesteryl ester transfer protein on the composition, size, and structure of spherical, reconstituted high density lipoproteins. *J. Biol. Chem.* **270**: 189–196.
27. Morrow, J. A., M. L. Segall, S. Lund-Katz, M. C. Phillips, M. Knapp, B. Rupp, and K. H. Weisgraber. 2000. Differences in stability among the human apolipoprotein E isoforms determined by the amino-terminal domain. *Biochemistry*. **39**: 11657–11666.
28. Krebs, K. E., J. A. Ibdah, and M. C. Phillips. 1988. A comparison of the surface activities of human apolipoproteins A-I and A-II at the air/water interface. *Biochim. Biophys. Acta.* **959**: 229–237.
29. Tüchsen, E., M. O. Jensen, and P. Westh. 2003. Solvent accessible surface area (ASA) of simulated phospholipid membranes. *Chem. Phys. Lipids.* **123**: 107–116.
30. Zorich, N., A. Jonas, and H. J. Pownall. 1985. Activation of lecithin cholesterol acyltransferase by human apolipoprotein E in discoidal complexes with lipids. *J. Biol. Chem.* **260**: 8831–8837.
31. Pind, S., A. Kuksis, J. J. Myher, and L. Marai. 1984. Resolution and quantitation of diacylglycerol moieties of natural glycerophospholipids by reversed-phase liquid-chromatography with direct liquid inlet mass-spectrometry. *Can. J. Biochem. Cell Biol.* **62**: 301–309.
32. Jonas, A., N. L. Zorich, K. E. Kézdy, and W. E. Trick. 1987. Reaction of discoidal complexes of apolipoprotein A-I and various phosphatidylcholines with lecithin cholesterol acyltransferase. Interfacial effects. *J. Biol. Chem.* **262**: 3969–3974.
33. Thurmond, R. L., S. W. Dodd, and M. F. Brown. 1991. Molecular areas of phospholipids as determined by <sup>2</sup>H NMR spectroscopy. Comparison of phosphatidylethanolamines and phosphatidylcholines. *Biophys. J.* **59**: 108–113.
34. Jonas, A., J. Hefele Wald, K. L. Harms Toohill, E. S. Krul, and K. E. Kézdy. 1990. Apolipoprotein A-I structure and lipid properties in homogeneous, reconstituted spherical and discoidal high density lipoproteins. *J. Biol. Chem.* **265**: 22123–22129.
35. Sana, D. A., K. H. Weisgraber, S. J. Russell, R. W. Mahley, D. Huang, A. Saunders, D. Schmechel, T. Wisniewski, B. Frangione, and A. D. Roses. 1994. Apolipoprotein E associates with beta amyloid peptide of Alzheimer's disease to form novel monofibrils. Isoform apoE4 associates more efficiently than apoE3. *J. Clin. Invest.* **94**: 860–869.
36. Wisniewski, T., E. M. Castano, A. Golabek, T. Vogel, and B. Frangione. 1994. Acceleration of Alzheimer's fibril formation by apolipoprotein E in vitro. *Am. J. Pathol.* **145**: 1030–1035.
37. Pitas, R. E., J. K. Boyles, S. H. Lee, D. Foss, and R. W. Mahley. 1987. Astrocytes synthesize apolipoprotein E and metabolise apolipoprotein E-containing lipoproteins. *Biochim. Biophys. Acta.* **917**: 148–161.
38. Nakai, M., T. Kawamata, T. Taniguchi, K. Maeda, and C. Tanaka. 1996. Expression of apolipoprotein E mRNA in rat microglia. *Neurosci. Lett.* **211**: 41–44.
39. Chiba, H., H. Akita, K. Tsuchihashi, S-P. Hui, Y. Takahashi, H. Fuda, H. Suzuki, H. Shibuya, M. Tsuji, and K. Kobayashi. 1997. Quantitative and compositional changes in high density lipoprotein subclasses in patients with various genotypes of cholesteryl ester transfer protein deficiency. *J. Lipid Res.* **38**: 1204–1216.
40. Brousseau, M. E., M. R. Diffenderfer, J. S. Millar, C. Nartsupha, B. F. Asztalos, F. K. Welty, M. L. Wolfe, M. Rudling, I. Björkhem, B. Angelin, et al. 2005. Effects of cholesteryl ester transfer protein inhibition on high-density lipoprotein subspecies, apolipoprotein A-I metabolism, and fecal sterol excretion. *Arterioscler. Thromb. Vasc. Biol.* **25**: 1057–1064.
41. Saito, H., P. Dhanasekaran, F. Baldwin, K. H. Weisgraber, S. Lund-Katz, and M. C. Phillips. 2001. Lipid binding-induced conformational change in human apolipoprotein E. Evidence for two lipid-bound states on spherical particles. *J. Biol. Chem.* **276**: 40949–40954.
42. Abia, R., Y. M. Pacheco, E. Montero, V. Ruiz-Gutierrez, and F. J. Muriana. 2003. Distribution of fatty acids from dietary oils into phospholipid classes of triacylglycerol-rich lipoproteins in healthy subjects. *Life Sci.* **72**: 1643–1654.
43. Rye, K-A., M. N. Duong, M. K. Psaltis, L. K. Curtiss, D. J. Bonnet, R. Stocker, and P. J. Barter. 2002. Evidence that phospholipids play a key role in pre-beta apoA-I formation and high-density lipoprotein remodeling. *Biochemistry*. **41**: 12538–12545.